

Study of Cu^{2+} and Gd^{3+} Doping Effect on Magneto-Optical Properties of Ni Zn Fe_2O_4 Spinel ferrites

Babasaheb E. Phunde¹, Limbraj S. Ravangave²

^{1,2}Physics Research Centre Shri Sant Gadge Maharaj College, Loha Dist. Nanded Maharashtra, India

ABSTRACT

This work is based on synthesis and study of magneto-Optical properties of $\text{Ni}_{0.4}\text{Zn}_{0.6}\text{Fe}_2\text{O}_4$, $\text{Ni}_{0.4}\text{Cu}_{0.3}\text{Zn}_{0.3}\text{Fe}_2\text{O}_4$ and $\text{Ni}_{0.4}\text{Cu}_{0.3}\text{Zn}_{0.3}\text{Gd}_{0.075}\text{Fe}_{1.925}\text{O}_4$ nano spinel ferrites. All samples of mixed spinel ferrites were successfully synthesized using sol-gel auto combustion technique. The structural, optical and magnetic properties are investigated by using X-ray Diffractometer, FTIR Spectrometer, Scanning Electron Microscope and Vibrating Sample Magnetometer (VSM) respectively. XRD data analysis confirmed that formation of nanocrystalline cubic spinel structure of prepared samples. The crystallite size of synthesized nanoparticles was in 35 to 45nm range. The lattice constant shows increase with substitution of Cu^{2+} and Gd^{3+} ions in the host of $\text{Ni}_{0.4}\text{Zn}_{0.6}\text{Fe}_2\text{O}_4$. The absorption bands in IR spectrum around 448.2331 cm^{-1} and 560.23 cm^{-1} are attributed to ν_1 and ν_2 frequencies respectively. This is concluded that nano material exhibit in the form of spinel ferrite structure. SEM image shows that spinel ferrites were systematically arranged in the form of wires of larger sized diameter. Band gap energy E_g obtained using UV-Visible absorption data was increased with Cu^{2+} and Gd^{3+} substitution. The values of magnetic field H_c and saturation magnetization M_s was increased with Cu^{2+} and Gd^{3+} substitution as compared to values of H_c and M_s for $\text{Ni}_{0.4}\text{Zn}_{0.6}\text{Fe}_2\text{O}_4$.

Keywords: Mixed spinel ferrite, Ni-Cu-Zn spinel, NiFe₂O₄UV, VSM

INTRODUCTION

Iron (Fe) based mixed spinel ferrites are extraordinary, key materials and used in field of electromagnetic devices such as in phase shifters, sensors, recording media, and in high-density data storage devices[1-4]. The spinel ferrite materials have been classified into normal spinel ferrite, inverse spinel ferrite, and mixed inverse spinel ferrite. The nickel ferrite (NiFe_2O_4 , NFO), was classed as inverse spinel structure, has gained much more attention because of its peculiar physical properties such as low-grade Curie temperature, high electrical resistivity, high permeability, low magnetostriction, etc. [5]. The main structural units in mixed spinel ferrites are divalent metal oxides and trivalent ferric oxide. The chemical formula for inverse spinel structure is $A[\text{B}_2]\text{O}_4$ where A is divalent cations like Mn, Zn, Cu, Ni, Cd etc. occupies at tetrahedral site and B is trivalent cation Fe^{3+} and occupies tetrahedral and octahedral sites respectively. The divalent metal ion can be replaced by other divalent metal ions and Fe^{3+} can also be replaced by other trivalent cations like Al, Cr, Gd, La etc. [6]. In case of mixed ferrites divalent metal ions occupied at A site and Fe^{3+} ions occupied in the A as well B sites [7-8].

Mixed ferrites ($\text{NiCuZn Fe}_2\text{O}_4$) exhibit vital magnetic, electric, dielectric and optical properties which made them extensively useful in technological and industrial applications such as magnetic storage in microwave dices [9]. Recently Rare Earth (RE) ion doped spinel ferrites in nano form have got extensive importance due to their tremendous applications such as in transformer core, in magnetic memory, in antenna rods in biomedical field, catalysis, and solar cells [10-11].

Various methods have been used in the synthesis of spinel ferrite nano particles. Most commonly the Sol-gel method [12], Co-precipitation method [13], Hydrothermal[14], Spray drying [15], etc. However these techniques requires sophisticated instruments however Sol-gel auto combustion technique is comparatively very economic and involve easy steps in preparation of mixed spinel ferrites [16-17]. Hence in present work a Sol-gel auto combustion technique have been used. The raw materials are in the form of Metal nitrates and citric acid were used as oxidizing salts and combustion fuel. All chemicals were of high purity analytical reagent grade [16]. In the view of various applications the present paper reported the synthesis of $\text{NiZnFe}_2\text{O}_4$, $\text{NiCuZnFe}_2\text{O}_4$ and Cu^{2+} doped, rare earth element (Gd^{3+}) doped

NiCuZnFe₂O₄ mixed nano spinel ferrites. The influence of Cu²⁺ and Gd³⁺ doping on structural optical and magnetic properties of NiZnFe₂O₄ were discussed and reported.

MATERIAL AND METHODS

Ni_{0.4}Zn_{0.6}Fe₂O₄, Ni_{0.4}Cu_{0.3}Zn_{0.3}Fe₂O₄ and Ni_{0.4}Cu_{0.3}Zn_{0.3}Gd_{0.075}Fe_{1.925}O₄ nano spinel ferrite particles were synthesized by using cost effective sol-gel auto combustion technique and citric acid is used as a fuel. The analytical grade (AR) nickel nitrate (Ni (NO₃)₂.6H₂O), copper nitrate (Cu (NO₃)₂.6H₂O), gadolinium nitrate (Gd (NO₃)₃.9H₂O), ferric nitrate (Fe (NO₃)₃.9H₂O), Zinc nitrate Zn(NO₃)₂.6H₂O and citric acid (C₆H₈O₇) were used as raw materials (99.9% pure) in proper proportion. The metal nitrates to citric acid ratio was taken as 1:3. Ammonia solution was added to maintain the pH 7. Temperature required for the synthesis of ferrite nanoparticles is kept around 110 °C. The as-synthesized powder is sintered at 800 °C for 4 hour. The sintered samples are characterized using X-ray diffractometer (XRD), Fourier Transmittance infrared spectrometer (FTIR), Scanning Electron Microscopy (SEM), UV-Visible spectrophotometer and Vibrating sample magnetometer (VSM). The data obtained is analyzed and reported in this report.

RESULTS AND DISCUSSION

Structural Properties

The XRD spectra of sintered samples are recorded over the range 2θ = 20-80 degree by using Mini Flex II X-ray Diffractometer. XRD patterns of these three spinel ferrites namely, Ni_{0.4}Zn_{0.6}Fe₂O₄, Ni_{0.4}Cu_{0.3}Zn_{0.3}Fe₂O₄ and Ni_{0.4}Cu_{0.3}Zn_{0.3}Gd_{0.075}Fe_{1.925}O₄ are shown in Figure 1. The XRD pattern exhibit (111), (220), (311), (222), (400), (422), (511) and (440) peak. The peaks in the XRD pattern are attributed to cubic spinel structure of all three samples. Similar cubic spinel structure for Ni_{0.4}Zn_{0.2}Mn_{0.4}Fe₂O₄ was reported in the literature [17]. However Ni_{0.4}Zn_{0.6}Fe₂O₄ sample show extra impurity peaks related to Zn metal in the 20° to 30° degree range. No impurity peaks are observed for the samples Ni_{0.4}Cu_{0.3}Zn_{0.3}Fe₂O₄ and Ni_{0.4}Cu_{0.3}Zn_{0.3}Gd_{0.075}Fe_{1.925}O₄ indicate that Cu, Zn, and Gd completely dissolve in the NiFe₂O₄ lattice. The intensity of (311) peak shows significant decrease with low content Gd³⁺ doping. The average grain size was calculated using well known Scherer's [18] formula (1),

$$D = \frac{0.94\lambda}{\beta \cos \theta} \text{----- (1),}$$

Here λ is the wavelength of the x-ray and β is the full width at half maximum intensity in radians.

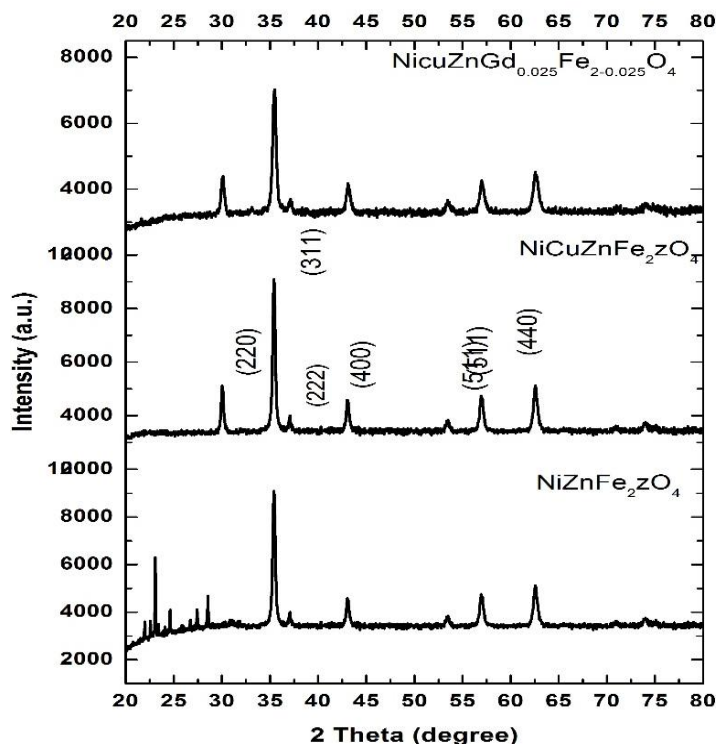


Figure 1. XRD pattern of Prepared three samples of spinel ferrites

The values of lattice constant 'a' (Å) for cubic sample [18] is determined by using the relation,

$$a = d_{hkl}(h^2 + k^2 + l^2) \text{----- (2)}$$

where (hkl) are the lattice constants. The unit cell volume (V) was calculated by using the following equation;

$$V = a^3 \text{----- (3)}$$

where, V is the unit cell volume a is the lattice constant. The X-ray density [19] (d_x) was calculated by using the following relation,

$$d_x = \frac{Z \times M}{V \times N_A} \text{ gm/cm}^3 \text{ -----(4)}$$

where, Z is the number of molecules per formula unit ($Z = 8$ for spinel system), M is molecular mass of the sample, $V = a^3$ is the unit cell volume and N_A is the Avogadro's number. The estimated crystallite size, lattice constant 'a', unit cell volume 'V' and X ray density were displayed in table 1. The effect of Cu^{2+} and Gd^{3+} doping on variation of structural parameters was clearly illustrated in the table 1.

Table 1: Estimated structural parameters from XRD Data

Sample Name	2θ (degree)	d (radians)	β (radians)	D (nm)	Lattice parameter 'a'	Volume (V)	X-ray Density
$\text{Ni}_{0.4}\text{Zn}_{0.6}\text{Fe}_2\text{O}_4$	35.600	2.5011	0.346	41	8.36	584.6	6.356
$\text{Ni}_{0.4}\text{Cu}_{0.3}\text{Zn}_{0.3}\text{Fe}_2\text{O}_4$	35.436	2.5311	0.400	38	8.4013	592.99	6.045
$\text{Ni}_{0.4}\text{Cu}_{0.3}\text{Zn}_{0.3}\text{Gd}_{0.075}\text{Fe}_{1.925}\text{O}_4$	35.360	2.5364	0.423	35	8.4122	595.3	6.072

Infrared (FTIR) Spectroscopy Investigations

IR spectrum of sample $\text{Ni}_{0.4}\text{Cu}_{0.3}\text{Zn}_{0.3}\text{Gd}_{0.075}\text{Fe}_{1.925}\text{O}_4$ scanned in the range 400 to 4000 cm^{-1} was presented in figure 2. The IR spectrum exhibits various vibrations corresponding to different functional groups. However absorption bands observed at 448.23 cm^{-1} and at 560.231 cm^{-1} which shows the characteristic bands of frequencies ν_2 and ν_1 related to intrinsic lattice vibrations of octahedral and tetrahedral coordination compounds of spinel ferrite structure respectively [23]. The peaks appeared around 880 cm^{-1} attributed to deformation of the iron oxide lattice into the bonding of Fe_3O_4 particles with surface OH groups. Similar results have been reported in the literature [24]. The absorption bands in the range 1600 cm^{-1} to 3400 cm^{-1} are attributed to stretchable vibration of the H–O–H group due to the presence of residual water [25]. The absorption peaks due to C–O and C–O₂ ion vibration are depicted in FTIR spectrum at around 1000 to 1500 cm^{-1} [26-27]. The FTIR spectrum reveals a peak at 1000 cm^{-1} that is reported in literature due to the incomplete decomposition of the products. Two prominent peaks appeared around $795\text{-}800 \text{ cm}^{-1}$ are attributed to (Gd–O) stretching vibrations [28].

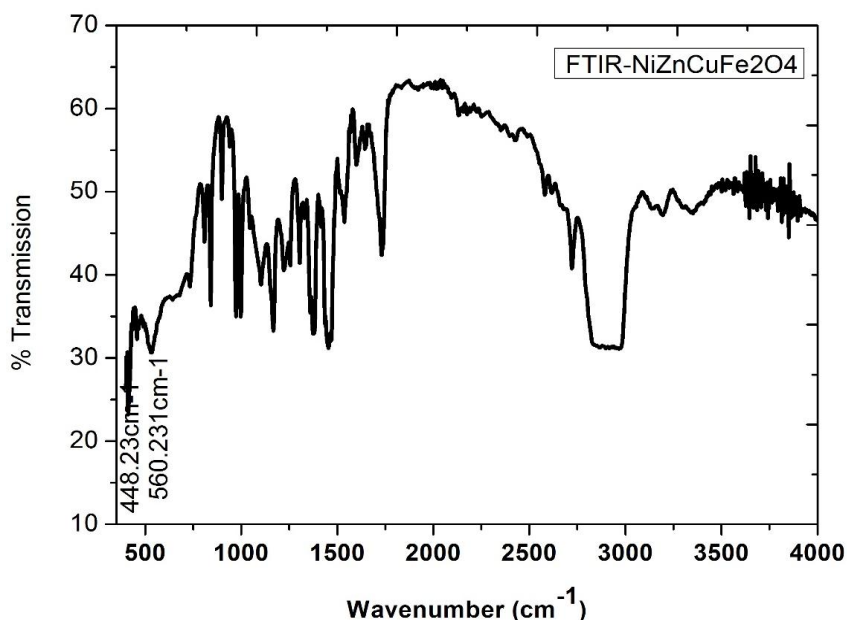


Figure 2. IR Spectrum of $\text{Ni}_{0.4}\text{Cu}_{0.3}\text{Zn}_{0.3}\text{Gd}_{0.075}\text{Fe}_{1.925}\text{O}_4$ of spinel ferrite

Surface Morphology Of $\text{Ni}_{0.4}\text{Cu}_{0.3}\text{Zn}_{0.3}\text{Gd}_{0.075}\text{Fe}_{1.925}\text{O}_4$ Spinel Ferrite

Figure 3 shows the SEM images of the $\text{Ni}_{0.4}\text{Cu}_{0.3}\text{Zn}_{0.3}\text{Gd}_{0.075}\text{Fe}_{1.925}\text{O}_4$ spinel. The SEM scan illustrate that micrograph composed of largely agglomerated nanoparticles of the sample. The large clusters of $\text{Ni}_{0.4}\text{Cu}_{0.3}\text{Zn}_{0.3}\text{Gd}_{0.075}\text{Fe}_{1.925}\text{O}_4$ ferrites formed by assembling of small spherical grains of nearly consistent in size. The spinel ferrites were systematically arranged. The dipole-dipole interactions among the uncapped nanoparticles results in agglomeration of nanosized particles.

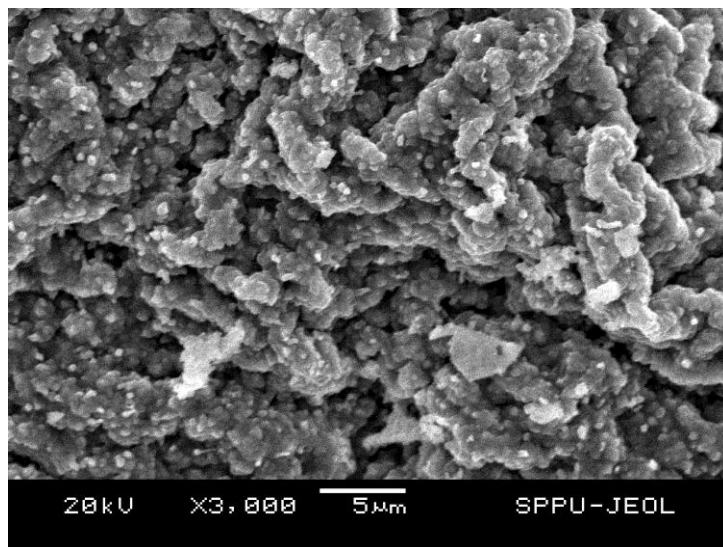


Figure 3. SEM image of $\text{Ni}_{0.4}\text{Cu}_{0.3}\text{Zn}_{0.3}\text{Gd}_{0.075}\text{Fe}_{1.925}\text{O}_4$ of spinel ferrite

Effect of Cu^{2+} and Gd^{3+} Doping On Absorption And Optical Band GAP

By using double distilled water as a solvent collide solution of prepared ferrites was prepared and absorption spectra was recorded in the range 200 to 800 nm by using Sistrionics Double Beam (2021) photo spectrometer. UV-Visible absorption spectra of $\text{Ni}_{0.4}\text{Zn}_{0.6}\text{Fe}_2\text{O}_4$, $\text{Ni}_{0.4}\text{Cu}_{0.3}\text{Zn}_{0.3}\text{Fe}_2\text{O}_4$ and $\text{Ni}_{0.4}\text{Cu}_{0.3}\text{Zn}_{0.3}\text{Gd}_{0.075}\text{Fe}_{1.925}\text{O}_4$ nano spinel ferrite was shown in figure 4.

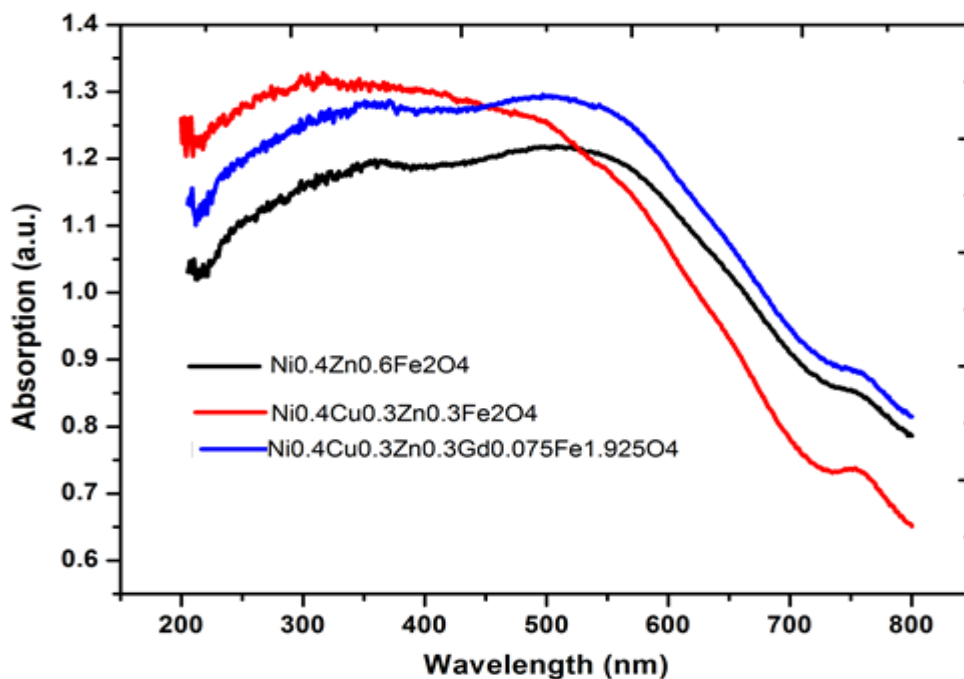


Figure 4. Absorption spectra of prepared spinel ferrite

The spectra show absorption at around 492 nm in the visible region for $\text{Ni}_{0.4}\text{Zn}_{0.6}\text{Fe}_2\text{O}_4$, ferrite sample similar results have reported by Elangbam C. Devi et al. (2017) in optical investigation of MnFe_2O_4 nanoferrites [28]. The absorption peak in visible region was shifted to lower side around 470 nm for $\text{Ni}_{0.4}\text{Cu}_{0.3}\text{Zn}_{0.3}\text{Fe}_2\text{O}_4$ doping of sample $\text{Ni}_{0.5}\text{Cu}_{0.5}\text{Zn}_{0.5}\text{Gd}_{0.075}\text{Fe}_{2-0.075}\text{O}_4$ and at around 467 nm for $\text{Ni}_{0.4}\text{Cu}_{0.3}\text{Zn}_{0.3}\text{Gd}_{0.075}\text{Fe}_{1.925}\text{O}_4$ sample on doping of Cu^{2+} and Gd^{2+} in $\text{Ni}_{0.4}\text{Zn}_{0.6}\text{Fe}_2\text{O}_4$. Spinel. The optical band gap energy (E_g) is estimated by using Tauc relation [12] as given below;

$$\alpha h\nu = B(h\nu - E_g)^n$$

where, α is the linear absorption coefficient of the material, B is the proportionality constant, h is Planck's constant (6.6260×10^{-34} J.s), ν is the photon energy, E_g is the optical energy band gap n is a constant associated with different kinds of electronic transitions ($n = 0.5$ for a direct allowed, $n = 2$ for an indirect allowed, $n = 1.5$ for a direct forbidden and $n = 3$ for an indirect forbidden). The Tauc plots for $\text{Ni}_{0.4}\text{Zn}_{0.6}\text{Fe}_2\text{O}_4$, $\text{Ni}_{0.4}\text{Cu}_{0.3}\text{Zn}_{0.3}\text{Fe}_2\text{O}_4$ and $\text{Ni}_{0.4}\text{Cu}_{0.3}\text{Zn}_{0.3}\text{Gd}_{0.075}\text{Fe}_{1.925}\text{O}_4$ are presented in figure 5.

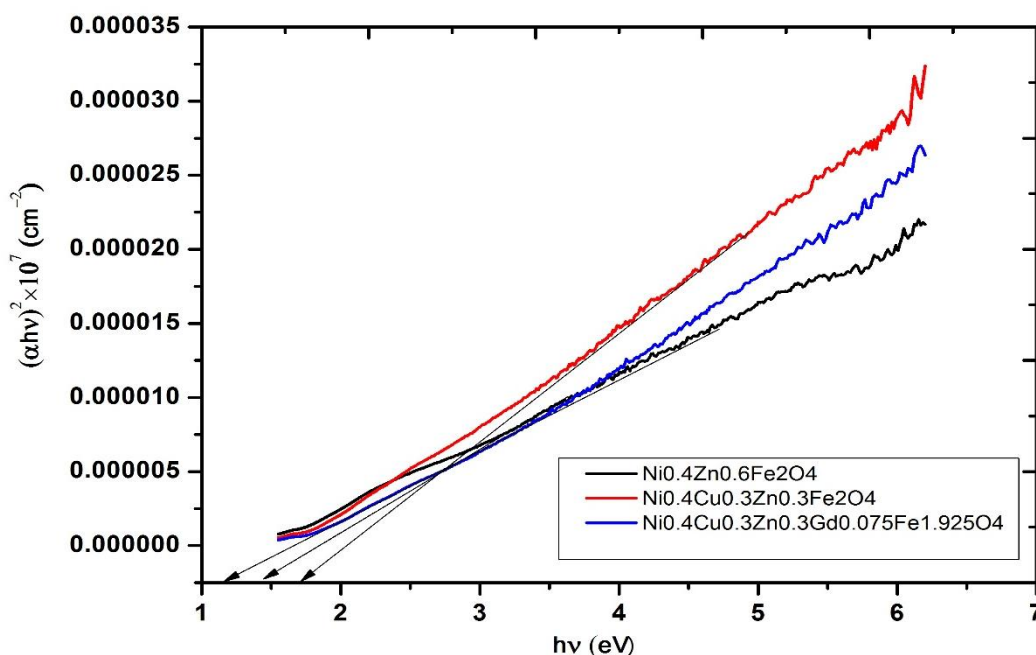


Figure 5. Tauc plots of spinel ferrite

The optical band gap estimated by using Tauc plots is presented in table 2. The band gap energy was increased on doping of Cu^{2+} for Zn^{2+} and Gd^{3+} for Fe^{3+} . The increase in band gap was related to decrease in crystallite size.

Magnetic Properties Prepared Spinel Ferrites

Vibrating sample magnetometer (VSM) technique was employed for magnetization measurement of $\text{Ni}_{0.4}\text{Zn}_{0.6}\text{Fe}_2\text{O}_4$, $\text{Ni}_{0.4}\text{Cu}_{0.3}\text{Zn}_{0.3}\text{Fe}_2\text{O}_4$ and $\text{Ni}_{0.4}\text{Cu}_{0.3}\text{Zn}_{0.3}\text{Gd}_{0.075}\text{Fe}_{1.925}\text{O}_4$ spinel ferrite samples. Figure. 6 shows the M-H plots of the samples.

The ferrite samples $\text{Ni}_{0.4}\text{Zn}_{0.6}\text{Fe}_2\text{O}_4$, $\text{Ni}_{0.4}\text{Cu}_{0.3}\text{Zn}_{0.3}\text{Fe}_2\text{O}_4$ and $\text{Ni}_{0.4}\text{Cu}_{0.3}\text{Zn}_{0.3}\text{Gd}_{0.075}\text{Fe}_{1.925}\text{O}_4$ exhibit narrow magnetic hysteresis loops which indicate the ferromagnetic behavior of these samples. Characteristics magnetic parameters such as saturation magnetization, remnant magnetization, coercivity and remanence ratio were measured from M-H loops and their values are given in Table 2. The results revealed that saturation magnetization and magnetic remanence were increased due to copper (Cu^{2+}) and Gadolinium (Gd^{3+}) doping in $\text{Ni}_{0.4}\text{Zn}_{0.6}\text{Fe}_2\text{O}_4$. However the values of magnetic remanence are very low and low coercivity this suggest that $\text{Ni}_{0.4}\text{Zn}_{0.6}\text{Fe}_2\text{O}_4$, $\text{Ni}_{0.4}\text{Cu}_{0.3}\text{Zn}_{0.3}\text{Fe}_2\text{O}_4$ and $\text{Ni}_{0.4}\text{Cu}_{0.3}\text{Zn}_{0.3}\text{Gd}_{0.075}\text{Fe}_{1.925}\text{O}_4$ are soft ferrite material, they can change easily their magnetization and work as magnetic conductors. These type of ferrites were useful in making magnetic cores for high frequency inductors, transformers and in many microwave devices [29]. This increase in M_s could be explained on the basis of Neel's model [30].

$$M = M_B - M_A \text{-----} (6)$$

Here, M_A and M_B represent the A and B sublattice magnetic moments in μ_B respectively. The total magnetic moment of ferromagnetic materials depends on the number of magnetic ions sharing at tetrahedral (A) and octahedral (B) positions

[19-20,]. In Ni-Zn-CuFe₂O₄ material, equal distribution of Fe³⁺ ions at tetrahedral and octahedral sites, whereas the octahedral sites are occupied by diatomic ions. However Gd³⁺ doped into Ni-Cu-Zn F₂O₄ lattice will result in the substitution of Gd³⁺ ions replacing the Fe³⁺ ions and Cu²⁺ at the B site in place of Zn²⁺. The magnetic moment of Cu²⁺ is large 1.7 Bohr Magnetron (B.M.) and that of Zn²⁺ is zero due to unpaired d¹⁰ electrons. The Gd³⁺ ions possess a large spin magnetic moment of 7.9 B.M. as compared to that of Fe³⁺ ion of 5M.B. [31]. Therefore, a small amount Cu²⁺ and Gd³⁺ substitution could lead to an increase in the total magnetic moment to enhance saturation magnetization.

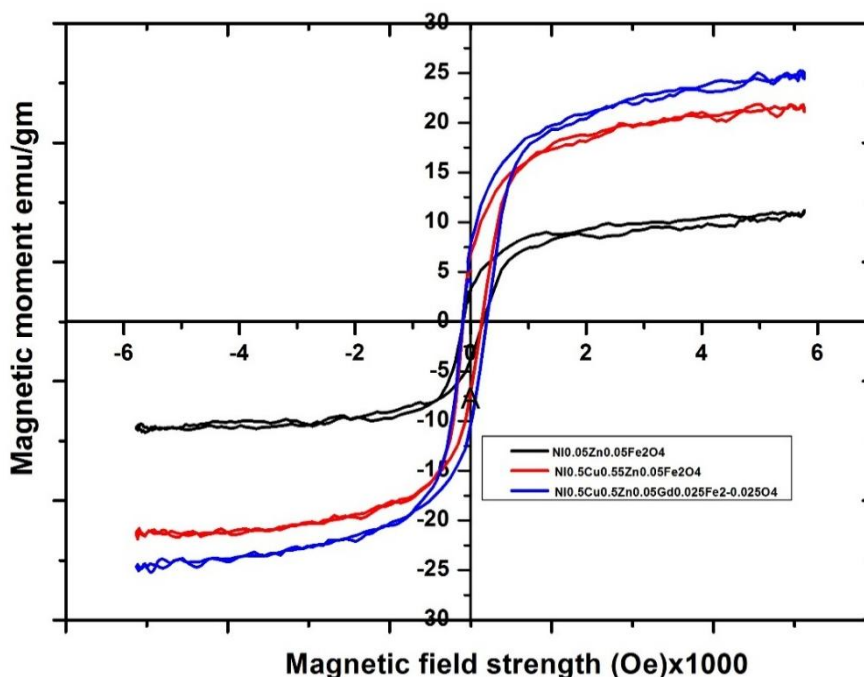


Figure 6. M-H plots of prepared spinel ferrite

Table 1: Estimated structural parameters from XRD Data

Sample	HC (Oe)	Ms (emu/gm)	Mr(emu/gm)	Ms/Mr	Band Gap (eV)
Ni _{0.4} Zn _{0.6} Fe ₂ O ₄	37.778	43.712	7.008	0.1603	1.25
Ni _{0.4} Cu _{0.3} Zn _{0.3} Fe ₂ O ₄	40	50.4960	8.1280	0.16096	1.46
Ni _{0.4} Cu _{0.3} Zn _{0.3} Gd _{0.075} Fe _{1.925} O ₄	50	49.2520	7.1680	0.14553	1.75

CONCLUSION

In Conclusion, Ni_{0.5}Cu_{0.5}Zn_{0.5}Fe₂O₄ and Ni_{0.5}Cu_{0.5}Zn_{0.5}Gd_{0.075}Fe_{2-0.075}O₄ mixed spinel ferrites were prepared via a sol-gel combustion method. XRD pattern revealed that formation of a cubic spinel ferrite structure. The substitution of Cu²⁺ and Gd³⁺ ions induced the marked influence that lattice parameter, unit cell volume and optical band gap were increased and X-ray density and crystalline size was decreased. Besides, the study indicated that Gd³⁺ doping had important impacts on the magnetic property of Ni_{0.5}Cu_{0.3}Zn_{0.3}Fe₂O₄ spinel ferrite. The saturation of magnetization, coercive field increased, and Remanence magnetization was decreased due to the effect of Cu²⁺ and Gd³⁺ doping, due to exchange interaction and redistribution of cations. The present work recommends that low content doping of Cu²⁺ and Gd³⁺ in Ni_{0.4}Zn_{0.6}Fe₂O₄ is useful for potential applications in multifunctional materials.

ACKNOWLEDGMENT

Authors are acknowledged to Principal, Shri Sant Gadge Maharaj College Loha and Dr. S.M. Rathod, Head Department of Physics Annasaheb Garware College Pune for Providing the Research centre and laboratory facilities.

REFERENCES

- [1]. J. A. Paiva, M. P. Graça, J. Monteiro, M. A. Macedo, and M. A. Valente, "Spectroscopy studies of NiFe₂O₄ nanosized powders obtained using coconut water," J. Alloys and Compounds, vol. 485, pp. 637–641, 2009.

- [2]. M. M. Krupa and I. V. Sharay, "Magnetic and magneto optical properties of Fe₃O₄ and NiFe₂O₄ nanoparticles," *Function. Mater.* vol. 21, pp 15, 2014.
- [3]. A. Hao, M. Ismail, S. He, N. Qin, R. Chen, A. M. Rana, D Bao, "Enhanced resistive switching and magnetic properties of Gd-doped NiFe₂O₄ thin films prepared by chemical solution deposition method," *Mater. Sci. Eng., B*, 229, pp86–95, 2018.
- [4]. W. Eerenstein, N. D. Mathur, J. F. Scott, "Multiferroic and magnetoelectric materials," *Nature* 442, pp759–765, 2006.
- [5]. U. Lüders, A. Barthélémy, M. Bibes, K. Bouzouhane, S. Fusil, E. Jacquet, J-P. Contour, J-F. Bobo, J. Fontcuberta, A. Fert, "NiFe₂O₄: A versatile spinel material brings new opportunities for spintronics". *Adv. Mater.* 18, pp.1733–1736, 2006.
- [6]. J. Smit, H.P.J. Wijn. *Ferrites*, Philips Technical Library, Eindhoven, 1959.
- [7]. A. M. Bhavikatti, S. kulkarni, A. Lagashetty, "Magnetic and transport properties of Cobalt ferrite", *International Journal of Electronic Engineering Research*, 2, pp. 125-134, 2010.
- [8]. P. I. Slick, *Ferrites for Non-Microwave Applications* North Holland, Amsterdam, Vol. 2, 1980.
- [9]. Hai-Bo Wang, Jin Hong Liu, Wen Fing Li, Jian-Bo Wang, Li Wang, Li-Jing Song, Shi-Jun Yuan, Fa-Shen Li, and F.S. Li, "Structural, dynamic magnetic and dielectric properties of Ni_{0.15}Cu_{0.2}Zn_{0.65}Fe₂O₄ ferrite produced by NaOH co-precipitation method", *J. Alloys Compd.*, 461 (1-2) pp373-377, 2010.
- [10]. R. N. Bhowmik, N. Naresh, "Structure, ac conductivity and complex impedance study of Co₃O₄ and Fe₃O₄ mixed spinel ferrites, *International Journal of Engineering, Science and Technology* 2, pp. 40-52, 2010., DOI: 10.4314/ijest.v2i8.63779
- [11]. I. Chicinas, "Soft magnetic nanocrystalline powders produced by mechanical alloying routes", *Journal of Optoelectronics and Advanced Materials*, 8, pp. 439-448, 2006.
- [12]. S. Zahi, M. Hashim, A.R. Daud, "Synthesis, magnetic properties and microstructure of Ni–Zn ferrite by sol–gel technique", *Journal of Magnetism and Magnetic Materials*, 308(2) pp177–182, 2007.
- [13]. I. H. Gul, W. Ahmed, A. Maqsood, "Electrical and magnetic characterization of nanocrystalline Ni–Zn ferrite synthesis by coprecipitation route", *Journal of Magnetism and Magnetic Materials*, 320(3-4) pp270–275, 2008.
- [14]. X. Jiao, D. Chen, Y. Hu, "Hydrothermal synthesis of nanocrystalline M_x(Zn_{1-x})Fe₂O₄ (M = Ni, Mn, Co; x = 0.40–0.60) powders", *Materials Research Bulletin*, 37(9) pp1583–1588, 2002.
- [15]. A. Takayama, M. Okuya, S. Kaneko, "Spray pyrolysis deposition of NiZn ferrite thin films, *Solid State Ionics*, 172(1–4), pp257-260, 2004.
- [16]. S. Balaji, K. Kalai Selvan, L. John Berchmans, et al, "Combustion synthesis and characterization of Sn⁴⁺ substituted nanocrystalline NiFe₂O₄", *Materials Science and Engineering B*, 119(2) pp119-124, 2005.
- [17]. K. Praveena and K. Sadhana, "Ferromagnetic Properties of Zn substituted Spinel Ferrites for High Frequency Applications", *International Journal of Scientific and Research Publications* 5(40) pp1-20, 2015. <http://ijsrp.org/>
- [18]. C. Kittel, P. Mc Euen, "Introduction to solid state physics", 8 323-324 New York: Wiley 1996.
- [19]. V. Chaudhari, S. E. Shirsath, M. L. Mane, R. H. Kadam, S. B. Shelke, D. R. Mane, "Crystallographic, magnetic and electrical properties of Ni_{0.5}Cu_{0.25}Zn_{0.25}La_xFe_{2-x}O₄ nanoparticles fabricated by sol-gel method", *J. Alloys Compd.*, 549 pp213–220, 213. DOI:10.1016/j.jallcom.2012.09.060
- [20]. Zen E-a., Validity of "vegard's law". *Mineralogical Society of America*; 1956.
- [21]. A. Manikandan, J. Judith Vijaya, M. Sundararajan, C. Meganathan, L. John Kennedy, M. Bououdina, "Optical and magnetic properties of Mg-doped ZnFe₂O₄ nanoparticles prepared by rapid microwave combustion method", *Superlattices and Microstructures*, 64, pp118–131, 2013.
- [22]. D. Domide, O. Walter, S. Behrens, E. Kaifer, and H.J. Himmel, "Synthesis of Heterobimetallic Zn/Co Carbamates: Single- Source Precursors to Nanosized Magnetic Oxides under Mild Conditions", *Eur. J. Inorg. Chem*, 2011(6) pp860-867, 2013.
- [23]. K. Kombaiaha, J. Judith Vijayaa, L. John Kennedy, M. Bououdina, R. Jothi Ramalingamd, Hamad A. Al-Lohedan, "Comparative investigation on the structural, morphological, optical, and magnetic properties of CoFe₂O₄ nanoparticles", *Ceramics International* 43 pp7682–7689, 2017 <http://dx.doi.org/10.1016/j.ceramint.2017.03.069>.
- [24]. Kryszewski M. and J. K. Jeszka) "Nanostructured conducting polymer composites-super paramagnetic particles in conducting polymers", *Synthetic Metals*, 94 pp99–104, 1998.
- [25]. Sonia, M. M. L., Blessi S., Pauline S. "Effect of copper substitution on the structural, morphological and magnetic properties of nickel ferrites", *International Journal of Research* 1 pp1051-1054, 2014.
- [26]. W. Zhang, A. Sun, X. Zhao, N. Suo, L. Yu, Z. Zuo, "Structural and magnetic properties of La³⁺ ion doped Ni–Cu–Co nano ferrites prepared by sol–gel auto-combustion method", *Journal of Sol-Gel Science and Technology*, 90 pp599-610, 2019.
- [27]. H. Nayaky, S. K. Pati and D. Bhatta, "Decomposition of γ - irradiated La₂(C₂O₄)₃ + CuO mixture: a non-isothermal study", *Radiation effects and defects in solids*, 159 pp93-106, 2014.
- [28]. N. Himansulal, "Kinetics Study on the Thermal Decomposition of Lanthanum Oxalate Catalysed by Zn-Cu Nano Ferrites", *Research Journal of Material Sciences*, 3(2) pp1-8, 2015.
- [29]. A. Okamoto, "The Invention of ferrites and their contribution to miniaturization of radios," *IEEE Globecom workshop Honolulu, HI, USA*, 1-6, 2015, doi10.1109/GLOCOMW2009.5360693

- [30]. M. Hoppe, S. Döring, M. Gorgoi, S. Cramm, M. Muller, “Enhanced ferrimagnetism in auxetic NiFe₂O₄ in the crossover to the ultrathin-film limit”, *Phys. Rev. B. Condens. Matter Mater. Phys.* pp91 054418, 2015.<http://dx.doi.org/10.1103/PhysRevB.91.054418>.
- [31]. K. Kamala K. Bharathi, P. N. , Santhosh, M. Pattabiraman, G. Markandeyulu, (2008) “Magneto capacitance in Dydoped Ni ferrite”. *Phys. Rev. B: Condens. Matter Mater. Phys.*, pp77 172401.<http://dx.doi.org/10.1103/PhysRevB.77.172401>.
- [32]. Kamala K. Bharathi, G. Markandeyulu, “Ferroelectric and ferromagnetic properties of Gd substituted nickel ferrite”, *J. Appl. Phys.* 103 pp07E309, 2015.<http://dx.doi.org/10.1063/1.2839281>.
- [33]. Huixue Yao, Xueer Ning, Hong Zhao, Aize Hao, and Muhammad Ismail, “Effect of Gd-Doping on Structural, Optical, and Magnetic Properties of NiFe₂O₄ As-prepared Thin Films via Facile Sol–Gel Approach”, *ACS Omega*, 6 pp6305-631, 2015., <http://dx.doi.org/10.1021/acsomega.0c06097>.